

Decentralized Control with Graph Neural Networks

Fernando Gama, Qingbiao Li, Ekaterina Tolstaya, Amanda Prorok, and Alejandro Ribeiro

Abstract—Dynamical systems consisting of a set of autonomous agents face the challenge of having to accomplish a global task, relying only on local information. While centralized controllers are readily available, they face limitations in terms of scalability and implementation, as they do not respect the distributed information structure imposed by the network system of agents. Given the difficulties in finding optimal decentralized controllers, we propose a novel framework using graph neural networks (GNNs) to learn these controllers. GNNs are well-suited for the task since they are naturally distributed architectures and exhibit good scalability and transferability properties. The problems of flocking and multi-agent path planning are explored to illustrate the potential of GNNs in learning decentralized controllers.

Index Terms—decentralized control, graph neural networks, graph signal processing, flocking, path planning

I. INTRODUCTION

Dynamical systems consist of a set of autonomous agents that seek to achieve a common goal or accomplish a global task [3, Ch. 3]. The agents can decide autonomously on the appropriate actions to take towards this global objective. Dynamical systems arise in many relevant scenarios such as path planning in multi-agent robotics [2], optimal power allocation in smart grids [4], estimation in sensor networks [5], or traffic coordination in smart cities [6]. The ability to control network dynamical systems thus becomes a technological problem of paramount importance [7], [8].

The autonomous nature of the each agent's action, coupled with the global character of the objective, creates a challenge in the design of control algorithms. That is, the action resulting from the controller needs to be executed separately at each agent but needs to be conducive to accomplishing the common goal. Thus, designing an appropriate controller requires solving this tension between local actions and a global objective.

One way to address this issue is to have a centralized unit receive the states of all agents, compute the appropriate control action that each agent should take, and transmit this action back to the agents. Different criteria can be chosen to decide on an appropriate action, like minimizing some given cost [9] or accounting for uncertainties [10]. *Centralized* controllers for network systems have been obtained for a vast array of problems including constrained consensus in multi-agent systems [11], load control in electrical grids [12], throughput control of wireless networks [13], or adaptive control in MIMO systems [14]. Centralized controllers, however, face

limitations in terms of scalability, since a single unit computes the actions of *all* agents in the team; implementation, since communication links between all agents and the centralized unit are required; and safety, since the system is vulnerable to attacks to this centralized unit.

Alternatively, the communication capabilities of the agents can be leveraged to compute a *decentralized* controller. Designing decentralized controllers demands relying on the communication network established by the agents that compose the system. These agents can communicate only with other nearby agents and exchange information with them. A decentralized controller, then, is built upon this distributed information structure. Furthermore, due to the inherent delay in the communication exchange, the information is not only distributed, but may also be outdated.

Optimal decentralized controllers are famously difficult to find [15]. Therefore, in this paper, we propose to *learn* suitable controllers from data. To do so, we adopt learning *models* that naturally respect the distributed information structure of the network system. More specifically, we study nonlinear maps between the local state and the control action given by two different types of graph neural networks (GNNs) [16], namely graph convolutional neural networks (GCNNs) [17]–[20] and graph recurrent neural networks (GRNNs) [6], [21], [22].

GNNs are information processing architectures built upon the notion of graph filters [23], so as to exploit the graph structure, and the use of nonlinearities to increase expressive power [24]. They are used to learn a nonlinear map between the state of the system and the action to be taken. In particular, GCNNs consist of a cascade of layers each of which applies a graph convolution followed by a pointwise nonlinearity [16]. GRNNs, on the other hand, model the dynamical evolution of the network data by learning a hidden state straight from data and using it to compute the action. In this way, the hidden state learns to keep track of the relevant past information as it pertains to the actions taken [22].

Both GCNNs and GRNNs process only local information (relied by neighboring agents) and can be computed in a distributed manner (each agent computes its corresponding output). Thus, using these architectures as parametrizations for learning nonlinear controllers leads naturally to decentralized solutions that are computationally simple. In this way, we can find the best parametrization within this family of architectures, knowing that the resulting controllers are always decentralized. Even though this is likely to yield a suboptimal controller, adopting these architectures facilitates the learning process by avoiding complex constraints that would otherwise be required to enforce the decentralized nature.

GCNN and GRNNs are not only local and distributed, making them computationally efficient, but also exhibit the properties of permutation equivariance and stability to perturbations [22], [25]. The former means that these architectures

The authors are supported by ARL DCIST CRA W911NF-17-2-0181. F. Gama, E. Tolstaya and A. Ribeiro are also supported by NSF CCF 1717120, ARO W911NF1710438, ISTC-WAS and Intel DevCloud. Q. Li and A. Prorok are also supported by EPSRC grant EP/S015493/1. F. Gama is with the Elect. Eng. Comput. Sci. Dept., Univ. of California, Berkeley, E. Tolstaya and A. Ribeiro are with the Dept. Elect. Syst. Eng., Univ. of Pennsylvania., and Q. Li and A. Prorok are with the Dept. Comput. Sci. Technol., Cambridge University. Email: fgama@berkeley.edu, {eig,aribeiro}@seas.upenn.edu, and {ql295,asp45}@cam.ac.uk. Preliminary discussions appear in [1], [2].

exploit the topological symmetries in the underlying network, while the latter implies the output is not significantly affected by small changes in the network structure. These results allow GCNNs and GRNNs to scale up, i.e. to be used in networks of increasing number of agents. These results also imply that these learning models transfer, i.e. they can be trained in one network and then transferred to another similar network, guaranteeing a certain level of performance. Also, GCNNs have enhanced discriminability capabilities when compared to linear distributed parametrizations [26].

Scalability and transferability become crucial properties when we train the models via *imitation learning* [27], [28]. In this framework, a training set comprised of optimal trajectories is available and the models learn to *imitate* these trajectories. The imitation learning framework rests on the availability of an optimal centralized controller which is only required during the offline training phase but is not needed during testing. For this reason, training architectures that scale and transfer is the key to learning decentralized controllers that are successful in previously unseen testing scenarios. In particular, we prove (Thm. 1) that the same set of parameters is optimal for all reordered instances of the same network, a property known as *permutation invariance* of the learned filters.

We begin Sec. II by formulating the problem of controlling dynamical systems and introducing the decentralized setting. In Sec. III we present graph filters (Sec. III-A), GCNNs (Sec. III-B) and GRNNs (Sec. III-C), and discuss imitation learning (Sec. III-D) as means of finding the optimal distributed controllers within each class. Sec. IV discusses the properties of permutation equivariance, stability and transferability of the aforementioned architectures and proves the permutation invariance of the optimal controller. This result plays a key role in explaining the observed scalability of GNN-based decentralized controllers. In Sec. V we show how to extend the GNN-based architectures to encompass time-varying communication networks; we present the particular case of a unit-delay scenario. We then illustrate the potential of GNN-based controllers learned by means of imitation learning in two different problems. In Sec. VI, we explore the problem of flocking [1], [29] where the objective is to coordinate a team of agents, initially flying at random velocities, to fly at the same velocity while avoiding collisions. Then, in Sec. VII we consider the problem of multi-agent path planning, where a team of robots needs to navigate a map to reach pre-specified targets in an efficient and collision-free manner. In both examples we show that GNN-based controllers exhibit very good performance while being computationally efficient, and we place special emphasis in the transferability and scalability of the learned controllers. We draw conclusions in Sec. VIII.

II. DECENTRALIZED CONTROLLERS

Consider a team of N agents $\mathcal{V} = \{v_1, \dots, v_N\}$. At time $t \in \{0, 1, 2, \dots\}$, each agent $v_i \in \mathcal{V}$ is described by a state $\mathbf{x}_i(t) \in \mathbb{R}^F$ and is equipped with the faculty of autonomously deciding on an action $\mathbf{u}_i(t) \in \mathbb{R}^G$. The collection of states of

all agents in the team can be compactly written as a matrix

$$\mathbf{X}(t) = \begin{bmatrix} \mathbf{x}_1(t)^\top \\ \vdots \\ \mathbf{x}_N(t)^\top \end{bmatrix} \in \mathbb{R}^{N \times F} \quad (1)$$

where each row corresponds to the state of each agent. Likewise, we can denote as $\mathbf{U}(t) \in \mathbb{R}^{N \times G}$ the collection of actions taken by all agents in the team at time t . These actions shape the value of the state of the team as determined by a dynamic model D

$$\mathbf{X}(t+1) = D\left(\{\mathbf{X}(\tau)\}_{\tau=0}^t, \{\mathbf{U}(\tau)\}_{\tau=0}^t\right) \quad (2)$$

This dynamic model is given by the physics of the system. One popular choice is a linear dynamic model [30], [31].

The general objective is to design control actions $\{\mathbf{U}(t)\}_t$ such that the resulting states $\{\mathbf{X}(t)\}$ minimize some cost function J

$$\{\mathbf{U}^*(t)\} = \underset{\{\mathbf{U}(t)\}: \mathbf{U}(t) \in \mathbb{R}^{N \times D}}{\operatorname{argmin}} J\left(\{\mathbf{X}(\tau)\}, \{\mathbf{U}(\tau)\}\right) \quad (3)$$

subject to the given dynamic model D [cf. (2)]. A popular choice of cost function is a quadratic cost, and a linear dynamic model coupled with such a quadratic cost is often referred to as an LQR problem [7, Ch. 8], [32].

The optimal control actions $\{\mathbf{U}^*(t)\}$ obtained from solving (3) for some loss function J , with no further constraint than some given dynamic model D [cf. (2)], are likely to be *centralized* control actions. This means that, in order to compute each individual action $\mathbf{u}_i(t)$, the agent may need access to the states $\{\mathbf{X}(\tau)\}$ of arbitrary agents in the team. In practice, this demands that all agents are in contact with each other, or that there exists some centralized unit to which all the agents send their state and then receive the corresponding optimal action to take. Both of these scenarios demand a more complex infrastructure, whether it is in terms of increased communication overhead, or the availability of a centralized computation unit. In what follows, our objective is to obtain *decentralized* controllers.

A decentralized controller is one that can be computed by relying only on information provided by other neighboring agents. We say that agents v_i and v_j are neighbors if there is a communication link between them. Typically, this communication link is given by their physical proximity. For example, if \mathbf{r}_i is the position of node v_i , then agents v_i and v_j can communicate if $\|\mathbf{r}_i - \mathbf{r}_j\| \leq R$ for some given communication radius R . We can conveniently describe the communication network using a graph $\mathcal{G} = (\mathcal{V}, \mathcal{E})$ where \mathcal{V} is the set of nodes, each one representing an agent, and $\mathcal{E} \subseteq \mathcal{V} \times \mathcal{V}$ is the set of edges, each one representing a communication link.

The decentralized controller can compute the action $\mathbf{u}_i(t)$ of agent v_i based only on the information provided by agents in its neighborhood, which we denote $\mathcal{N}_i = \{v_j \in \mathcal{V} : (v_j, v_i) \in \mathcal{E}\}$. We can then define this information as

$$\mathcal{X}_i(t) = \{\mathbf{x}_j(\tau) : v_j \in \mathcal{N}_i \cup v_i, \tau = 0, 1, \dots, t\} \quad (4)$$

which is the history of the state values of all neighboring agents across time. We can then define the optimal decentralized controller as the one that solves [cf. (3)]

$$\begin{aligned} \min_{\mathbf{U}, \Phi} J(\{\mathbf{X}(\tau), \{\mathbf{U}(\tau)\}\}) \\ \text{subject to } \mathbf{u}_i(t) = \Phi(\mathcal{X}_i(t)) \end{aligned} \quad (5)$$

for some function Φ . Note that, for the resulting problem to be truly decentralized, the state of each agent cannot depend on any global parameter either.

Assumption 1 (Locality of states). *The dynamical model D is such that $\mathbf{x}_i(t) = f(\mathcal{X}_i(t-1))$ for some function f , for all $i : v_i \in \mathcal{V}$; and with $\mathcal{X}_i(-1) = \{\mathbf{x}_i(0)\}$.*

Asn. 1 determines that the state $\mathbf{x}_i(t)$ of agent i at each time instant t depends only on the agent's own measurements and/or those obtained from immediate neighbors. This assumption is not difficult to satisfy, as we show in Secs. VI and VII, yet care is required in selecting the observation model within the specific dynamic [cf. (2)].

Solving the optimal decentralized controller problem (5) over the space of all functions Φ mapping the neighbor history (4) to the control action is famously difficult to do [15]. As a matter of fact, even for a LQR problem with distributed constraints, the resulting decentralized optimal controller is nonlinear. Thus, we propose to adopt a nonlinear parametrization of Φ that is naturally local and distributed, so that the resulting controller is always decentralized. Namely, graph neural networks [33].

III. GRAPH NEURAL NETWORKS

Optimal decentralized controllers are difficult to find due to the constraint in (5) that forces the controller to be a function only of neighboring information. To address this, we propose to parametrize $\mathbf{U}(t) = \Phi(\mathcal{X}_i(t))$ with a function Φ that is naturally distributed, so that the constraint is always satisfied. Thus, instead of considering the space of all possible functions with the additional constraint of a distributed formulation, we restrict our attention to controllers that can be computed by means of a graph neural network (GNN). While the obtained solutions are likely to be suboptimal, they are easy to train, can be computed in a distributed manner and exhibit several properties that make them a reasonable choice of parametrization, besides playing a key role in the practical success observed in Secs. VI and VII. In short, we restrict the functional optimization problem (5) to be a parameter optimization problem over the space of GNNs, which are nonlinear, local and distributed.

We introduce the framework of graph signal processing (GSP) and the fundamental concept of graph filters, allowing for a straightforward mathematical description of the decentralized nature of the data and how to process it in a linear manner (Sec. III-A). Graph convolutional neural networks (GCNNs) build upon graph filters by adding pointwise nonlinearities to conform a layer, and cascading several layers as means of increasing their representation power, i.e. the space of functions that they can describe (Sec. III-B). Graph recurrent neural networks (GRNNs) further incorporate the

time structure by learning a sequence of *hidden* states that keep track of the relevant information in the system evolution (Sec. III-C). Finally, we introduce imitation learning as a way of training these architectures to learn useful decentralized controllers (Sec. III-D).

A. Graph filters

The distributed nature of the decentralized controllers comes from the fact that each agent can only communicate with other nearby agents. As discussed in Sec. II, we describe this communication network by means of a graph $\mathcal{G} = (\mathcal{V}, \mathcal{E})$, where \mathcal{V} is the set of nodes (agents) and \mathcal{E} is the set of edges (communication links). A decentralized controller, thus, is only allowed to process information that propagates through this graph. We use graph signal processing (GSP) [34]–[36] as the appropriate framework to learn such controllers.

A *graph signal* $\mathbf{x} : \mathcal{V} \rightarrow \mathbb{R}$ is defined as a function that assigns a scalar value to each node and can be conveniently described by a vector $\mathbf{x} \in \mathbb{R}^N$ where $[\mathbf{x}]_i = x_i$ is the signal value assigned to node v_i , $x(v_i) = x_i$. We can extend this concept to describe the collection of states of all agents in the team $\mathbf{X} \in \mathbb{R}^{N \times F}$ [cf. (1)], by assigning a F -dimensional vector to each agent $\mathbf{X} : \mathcal{V} \rightarrow \mathbb{R}^F$ so that $\mathbf{X}(v_i) = \mathbf{x}_i \in \mathbb{R}^F$. We can thus interpret each column of the matrix \mathbf{X} as a separate graph signal $\mathbf{x}^f \in \mathbb{R}^N$ where $[\mathbf{x}^f]_i = x_i^f$ is the value of the f th graph signal at node v_i , for $f = 1, \dots, F$. For ease of exposition, we refer to \mathbf{X} as a graph signal as well, even though, technically, \mathbf{X} is a collection of F graph signals.

A graph signal $\mathbf{X} : \mathcal{V} \rightarrow \mathbb{R}^F$ contains information only about the nodes in the graph \mathcal{G} , but bears no relation with the edge set \mathcal{E} that determines the topology of the graph. This information is captured in another matrix $\mathbf{S} \in \mathbb{R}^{N \times N}$ which is a description of the *support* of the graph and satisfies $[\mathbf{S}]_{ij} = s_{ij} = 0$ whenever $i \neq j$ or $(v_j, v_i) \notin \mathcal{E}$. Note that the support matrix \mathbf{S} respects the sparsity of the graph since there is a zero entry whenever agents v_i and v_j do not share a communication link between each other. Examples of the support matrix typically used in the literature include the adjacency matrix [34], the Laplacian matrix [35], the Markov matrix [37], as well as normalized counterparts [18], [19].

The fact that the support matrix \mathbf{S} respects the sparsity of the graph is the key property that allows it to conveniently describe distributed operations in a straightforward manner. To see this, consider the linear operation $\mathbf{S}\mathbf{X}$ that results from applying the support matrix \mathbf{S} to a graph signal \mathbf{X} . The output is another graph signal whose (i, f) th entry is computed as

$$[\mathbf{S}\mathbf{X}]_{if} = \sum_{j=1}^N [\mathbf{S}]_{ij} [\mathbf{X}]_{jf} = \sum_{j: v_j \in \mathcal{N}_i} s_{ij} x_j^f \quad (6)$$

where $\mathcal{N}_i = \{v_j \in \mathcal{V} : (v_j, v_i) \in \mathcal{E}\}$ is the set of neighbors of v_i . The operation $\mathbf{S}\mathbf{X}$ acts as a diffusion operator that *shifts* the information contained in the state \mathbf{X} across the graph, thus oftentimes \mathbf{S} receives the name of *graph shift operator* (GSO).

The second equality in (6) holds due to the sparsity pattern of the support matrix \mathbf{S} , that is, there are nonzero entries only when $(v_j, v_i) \in \mathcal{E}$. This implies that the graph signal that results from the linear operation $\mathbf{S}\mathbf{X}$ requires local information

that is provided by neighboring nodes only. Likewise, each node can separately compute this output without knowledge of the rest of the graph, only knowing their one-hop neighbors. In essence, $\mathbf{S}\mathbf{X}$ is a *local* and *distributed* operator, and thus serves as the building block for learning *decentralized* controllers.

A finite-impulse response (FIR) graph filter $\mathbf{H} : \mathbb{R}^{N \times F} \rightarrow \mathbb{R}^{N \times G}$ maps a graph signal $\mathbf{X} \in \mathbb{R}^{N \times F}$ into another one $\mathbf{Y} \in \mathbb{R}^{N \times G}$ by means of a polynomial in the support matrix

$$\mathbf{Y} = \sum_{k=0}^K \mathbf{S}^k \mathbf{X} \mathbf{H}_k = \mathbf{H}(\mathbf{X}; \mathbf{S}, \mathcal{H}) \quad (7)$$

where $\mathcal{H} = \{\mathbf{H}_k \in \mathbb{R}^{F \times G}, k = 0, \dots, K\}$ is the set of *filter coefficients*, *filter weights* or *filter taps*. Conceptually, a graph filter of the form (7) can be understood as an application of a bank of FG filters to each of the F graph signals \mathbf{x}^f that form the columns of \mathbf{X} and aggregating the corresponding outputs. To see this, note that \mathbf{y}^g , the g th column of the graph signal \mathbf{Y} , can be obtained as

$$\mathbf{y}^g = \sum_{f=1}^F \mathbf{y}^{gf} \text{ with } \mathbf{y}^{gf} = \sum_{k=0}^K h_k^{fg} \mathbf{S}^k \mathbf{x}^f \quad (8)$$

where $h_k^{fg} = [\mathbf{H}_k]_{fg}$ is the (f, g) th entry of the k th filter tap. A filter of the form (7) inherits the name of FIR filter from its discrete-time counterpart. To see this, note that a discrete-time signal can be described within the GSP framework as being supported by a directed cycle graph. By adopting a support matrix \mathbf{S} such that $[\mathbf{S}]_{i(i-1)} = 1$ and 0 elsewhere, \mathbf{y}^{gf} in (8) becomes a regular circular convolution, i.e. $[\mathbf{y}^{gf}]_n = \sum_{k=0}^K h_k^{fg} [\mathbf{x}^f]_{n-k+1}$. Therefore, when considering graph signals defined on a directed cycle graph support (i.e. discrete-time signals), (8) boils down to a regular convolution, and thus (7) becomes a bank of FIR filters [38].

FIR graph filters (7) are local and distributed mappings between graph signals. They are local since they only require communication exchanges with one-hop neighbors. Note that $\mathbf{S}^k = \mathbf{S}(\mathbf{S}^{k-1})$ and thus $\mathbf{S}^k \mathbf{X}$ can be computed by communicating k -times with one-hop neighbors and aggregating the transmitted information. On the other hand $\mathbf{X} \mathbf{H}_k$ is a linear combination of the rows of \mathbf{X} which are the F state values for each of the nodes, not requiring any communication between agents. In short, multiplications of \mathbf{X} by the right have to respect the sparsity of the graph, since they mix values across different nodes, while multiplications of \mathbf{X} by the left can be arbitrary, since they only mix state values within the same node (in a weight-sharing scheme). FIR graph filters are distributed since each node can compute the output of the filter separately, by aggregating the information shared K times by their one-hop neighbors, and then weighing this information by the filter taps contained in \mathbf{H}_k . Thus, there is no need for the nodes to know \mathbf{S} (or the entire graph) at implementation time, they only need to know their one-hop neighbors \mathcal{N}_i , and the corresponding filter taps \mathcal{H} .

Remark 1 (Choice of \mathbf{S}). The choice of support matrix \mathbf{S} affects the performance of the resulting controller, and thus different alternatives exhibit different desirable properties [39]. However, no single choice has been shown to outperform

others in a wide range of problems, and thus we keep a generic support matrix \mathbf{S} that acts as a stand-in for any matrix that respects the sparsity of the graph. The results we obtain in this paper hold for any problem-specific choice of support matrix.

B. Graph convolutional neural networks

Graph filters (7) are linear maps between graph signals, and as such, are only able to capture linear relationships if used to design decentralized controllers. However, it is known that these controllers are typically nonlinear [15]. Therefore, we need a map that is capable of capturing nonlinear relationships if we are to design successful decentralized controllers.

Graph convolutional neural networks (GCNNs) are a cascade of operational blocks or *layers*, each of which applies a graph filter (7) followed by a pointwise nonlinearity [17], [18], [20]. Let $\mathbf{X}_\ell \in \mathbb{R}^{N \times F_\ell}$ be the signal obtained at the output of layer ℓ . This output is computed as

$$\mathbf{X}_\ell = \sigma(\mathbf{H}_\ell(\mathbf{X}_{\ell-1}; \mathbf{S}, \mathcal{H}_\ell)) \quad (9)$$

where $\mathbf{H}_\ell : \mathbb{R}^{N \times F_{\ell-1}} \rightarrow \mathbb{R}^{N \times F_\ell}$ is a graph filter of the form (7) described by the set of filter coefficients $\mathcal{H}_\ell = \{\mathbf{H}_{\ell k} \in \mathbb{R}^{F_{\ell-1} \times F_\ell}, k = 0, \dots, K_\ell\}$, and $\sigma : \mathbb{R} \rightarrow \mathbb{R}$ is a nonlinear function that, in an abuse of notation, is used in (9) to denote its element-wise application to the entries of the output of the graph filter. The input \mathbf{X}_0 to the first layer is the data, $\mathbf{X}_0 = \mathbf{X}$, and we collect the output at the last layer

$$\Phi(\mathbf{X}; \mathbf{S}, \mathcal{H}) = \mathbf{X}_L \quad (10)$$

to be the output of the GCNN Φ , and where $\mathcal{H} = \{\mathcal{H}_\ell, \ell = 1, \dots, L\}$ is the set of all filter taps used in all layers. The number of layers L , the number of features per layer F_ℓ , the order of each graph filter K_ℓ , and the nonlinear function σ are all design choices, and are normally called *hyperparameters* (in contrast to the filter taps, that often receive the name of parameters). In this respect, traditional techniques of hyperparameter selection hold for GCNNs as well [40].

GCNNs extend graph filters by adding pointwise nonlinearities and cascading several operational blocks. Thus, they retain many of the properties that graph filters exhibit. Mainly, GCNNs are also local and distributed architectures, since the nonlinearities are applied individually at each node and for each state value, without compromising the local and decentralized nature of graph filters. Therefore, GCNNs are suitable choices for learning nonlinear decentralized controllers.

Remark 2 (Implementations of graph convolutions). Several implementations of GCNNs have been proposed. These include graph convolutional filters (7) implemented in the spectral domain [17], with Chebyshev polynomials [18] and with ordinary polynomials [20]. One can also encounter GNNs described in terms of local aggregation functions [19], [41], which can be seen as particular cases of GCNNs (9) that use graph filters of order $K_\ell = 1$, resulting in a parametrization with lower representation power than those in [17], [18], [20]. It is important to point out that the GCNN implementations in [17], [18], [20] are equivalent in the sense that they span the exact same set of possible maps. Thus, although we use the polynomial description of [20], the results we present

apply irrespectively of implementation. The architectures in [19], [41], being restricted to filters of order $K_\ell = 1$, span a subset of the maps that can be represented by the more generic GCNNs in [17], [18], [20]. While, technically, [19], [41] are possible options, we note that high discriminability filters require the use of higher order graph filters [25]. Equivalence notwithstanding, different architectures may differ in their ease of training and, consequently, may lead to different performance in practice; albeit, no particular implementation has shown better performance across a wide range of applications.

Remark 3 (Practical differences with regular CNNs). While, so far, we have presented GCNNs (9) as extensions of graph filters (7) obtained by the inclusion of pointwise nonlinearities, GCNNs can also be thought of as extensions of regular convolutional neural networks (CNNs) [42]. In practice, CNNs usually include two further operations that are observed to improve their performance. First, CNNs often include a pooling operation after (sometimes, before) the application of the nonlinearity. [43, Ch. 9]. Pooling consists of sampling followed by a summarizing function, in order to reduce the dimensionality of the signal as it progresses through the layers. While several methods for sampling graph signals exist [44], [45], these methods become less relevant in the context of physical networks since each agent has computational power. Thus, the dimensionality reduction brought around by pooling is not strictly necessary. In any case, pooling schemes for GCNNs that respect the topology of the physical network are presented in [20]. Second, CNNs usually include a fully-connected neural network [43, Ch. 6] at the end of the convolutional layers. Fully-connected layers, however, violate the decentralized nature of GCNNs, and thus are not considered in the description (9)-(10).

C. Graph recurrent neural networks

Graph recurrent neural networks (GRNNs) are nonlinear information processing architectures better suited for handling graph processes (i.e. sequences of graph signals) [46]–[49] since they exploit both the graph and time structure of data [6], [21], [22]. A GRNN learns to extract information from the sequence $\{\mathbf{X}(t)\}$ in the form of a sequence of *hidden states* $\{\mathbf{Z}(t)\}$. Each hidden state is a graph signal $\mathbf{Z}(t) \in \mathbb{R}^{N \times H}$ and is learned from the input process by using a nonlinear map that takes the current data point $\mathbf{X}(t)$ and the previous hidden state $\mathbf{Z}(t-1)$ as inputs, and outputs the updated hidden state $\mathbf{Z}(t)$. This map is parametrized as

$$\mathbf{Z}(t) = \sigma(\mathbf{A}(\mathbf{X}(t); \mathbf{S}, \mathcal{A}) + \mathbf{B}(\mathbf{Z}(t-1); \mathbf{S}, \mathcal{B})) \quad (11)$$

where $\mathbf{A} : \mathbb{R}^{N \times F} \rightarrow \mathbb{R}^{N \times H}$ and $\mathbf{B} : \mathbb{R}^{N \times H} \rightarrow \mathbb{R}^{N \times H}$ are graph filters (7) characterized by the set of filter taps $\mathcal{A} = \{\mathbf{A}_k \in \mathbb{R}^{F \times H}, k = 0, \dots, K\}$ and $\mathcal{B} = \{\mathbf{B}_k \in \mathbb{R}^{H \times H}, k = 0, \dots, K\}$, respectively. The function $\sigma : \mathbb{R} \rightarrow \mathbb{R}$ is a pointwise nonlinearity that is applied elementwise to the graph signal that results from adding up the two filter outputs.

A controller can be learned from the hidden state by means of another nonlinear map

$$\mathbf{U}(t) = \rho(\mathbf{C}(\mathbf{Z}(t); \mathbf{S}, \mathcal{C})) \quad (12)$$

where $\mathbf{C} : \mathbb{R}^{N \times H} \rightarrow \mathbb{R}^{N \times G}$ is a graph filter (7) characterized by the filter taps $\mathcal{C} = \{\mathbf{C}_k \in \mathbb{R}^{H \times G}, k = 0, \dots, K_o\}$, and where $\rho : \mathbb{R} \rightarrow \mathbb{R}$ is a pointwise nonlinearity that is applied to each entry of the output of the filter. In the case of a GRNN (11)-(12), the design hyperparameters are the size of the hidden state H , the order of the filters K in (11) and K_o in (12), and the choice of nonlinearities σ and ρ .

GRNNs (11)-(12) are local and distributed architectures, since they are the composition of graph filters (7), that exhibit these properties, and pointwise nonlinearities, that do not alter them. Oftentimes, we choose $K_o = 0$ so that the output controller (12) is obtained by combining the hidden state values at each node, saving on communication cost and avoiding delays [cf. (7)]; in other words, the communication with one-hop neighbors is carried out by (11) and used to learn an appropriate hidden state. In any case, GRNNs are also suitable choices for learning nonlinear decentralized controllers.

We note that the number of parameters in \mathcal{A} , \mathcal{B} , and \mathcal{C} is independent of both N the size of the graph and the length of the sequence. Thus, GRNNs can seamlessly adapt to arbitrarily long sequences, albeit they might require gating mechanisms to improve training [22].

D. Imitation learning

To learn a successful decentralized controller by means of a graph filter (7), a GCNN (9)-(10) or a GRNN (11)-(12), we need to determine the appropriate set of filter taps (also known as parameters). This is typically achieved by means of training, which is an optimization procedure that attempts to find the best filter taps for a given criterion, and a given *training set* [50]. This set contains example trajectories of the state of the system that are leveraged to determine the best controller according to the given criterion. One popular approach to training controllers is *reinforcement learning* [51]. In what follows, and exploiting the scalability of the proposed parametrizations, we adopt, instead, a much simpler method known as *imitation learning* [27], [28].

Imitation learning assumes the availability of a training set \mathcal{T} comprised of pairs of trajectories $(\mathbf{X}(t), \mathbf{U}^*(t))_t$, where $\mathbf{U}^*(t)$ is some optimal, often centralized, controller trajectory¹. Then, we train the filter taps to minimize the distance between the resulting controller and the optimal one

$$\mathcal{H}^* = \underset{\mathcal{H}}{\operatorname{argmin}} \sum_{(\mathbf{X}(t), \mathbf{U}^*(t))_t \in \mathcal{T}} \sum_t \|\Phi(\mathbf{X}(t)) - \mathbf{U}^*(t)\| \quad (13)$$

where Φ is a stand-in for either a graph filter (7), a GCNN (9)-(10), or a GRNN (11)-(12), and where \mathcal{H} is a stand-in for the corresponding filter taps.

First and foremost, we note that the optimal controller is only required at *training time*, but not at *testing time*, when the trained controller is actually being deployed. In this respect, the decentralized nature of the resulting, trained

¹This controller need not be optimal, as it may be obtained through an approximate heuristic. What we assume is that this controller exhibits a significantly good performance and tends to be difficult to compute –either because it is centralized, it is computationally costly or does not scale. We retain the label *optimal* for ease of exposition.

controller, is not violated. Second, centralized (sub-)optimal controllers are often available [29], [52], albeit they rarely scale to large teams. Thus, exploiting the scalability of the chosen parametrizations, we are able to train the controllers in a relatively small graph, and then successfully employ it on larger teams. Thus, the computational cost of obtaining a centralized controller can be managed by considering small teams at training time. Third, the transferability of the chosen parametrizations also plays a key role, since we know that the trained controllers still work well when being deployed on slightly different scenarios than the ones observed in training.

IV. PERMUTATION INVARIANCE

We leverage imitation learning (13) to find the the optimal filter taps \mathcal{H}^* for the chosen parametrization Φ of the decentralized controller. When we train, we typically assume a given \mathbf{S} , and the trajectories that compose the training set are all defined over the same \mathbf{S} . However, due to the requirement to use a centralized optimal controller $\mathbf{U}^*(t)$ during training, \mathbf{S} may actually not be the same one that is used during deployment. Thus, we need some kind of guarantees on whether the coefficients learned by means of solving (13) are still useful when changing \mathbf{S} .

For any given set of filter taps \mathcal{H} , we can adapt the resulting graph filter to any \mathbf{S} . That is, the filter taps \mathcal{H} are decoupled from \mathbf{S} in (7), and we can use the same \mathcal{H} for different values of \mathbf{S} . Furthermore, we can use the same filter taps \mathcal{H} for different graph sizes, since \mathbf{H}_k is independent of N . The same holds for GCNNs and GRNNs, since they are built upon graph filters. Now, the fact that we *can* use the same filter taps \mathcal{H} on any graph, does not imply that doing so would yield good transference performance.

To characterize cases where we do expect good transference performance, we show here that the optimal set of filter taps \mathcal{H}^* is invariant to permutations. Let \mathcal{P} be the set of all permutation matrices

$$\mathcal{P} = \{\mathbf{P} \in \{0, 1\}^{N \times N} : \mathbf{P}\mathbf{1} = \mathbf{1}, \mathbf{P}^\top \mathbf{1} = \mathbf{1}\}. \quad (14)$$

That is, $\mathbf{P} \in \mathcal{P}$ is a binary matrix with a single nonzero entry in each column and each row. When applied to a graph signal $\mathbf{P}^\top \mathbf{X}$ it amounts to a reordering of its rows, which means a reordering of the node labels. Likewise, $\mathbf{P}^\top \mathbf{S} \mathbf{P}$ stands for the corresponding reordering of the underlying support matrix.

The following theorem states that if the set of filter taps \mathcal{H}^* are optimal for a given \mathbf{S} , then they are optimal for all node reorderings of \mathbf{S} .

Theorem 1 (Permutation Invariance). *Let \mathbf{S} be a given support matrix, and let $\mathcal{T} = \{(\mathbf{X}(t), \mathbf{U}^*(t))_t\}$ be a given training set of trajectories defined over \mathbf{S} , with $\mathbf{X}(t)$ satisfying Asn. 1. Let \mathcal{H}^* be the optimal set of filter taps that solve the imitation learning problem (13) for a chosen parametrization Φ*

$$\mathcal{H}^* = \underset{\mathcal{H}}{\operatorname{argmin}} \sum_{(\mathbf{X}(t), \mathbf{U}^*(t))_t \in \mathcal{T}} \sum_t \left\| \Phi(\mathbf{X}(t); \mathbf{S}, \mathcal{H}) - \mathbf{U}^*(t) \right\|. \quad (15)$$

Let $\hat{\mathbf{S}} = \mathbf{P}^\top \mathbf{S} \mathbf{P}$ for any permutation matrix $\mathbf{P} \in \mathcal{P}$ [cf. (14)], and let $\hat{\mathcal{T}} = \{(\hat{\mathbf{X}}(t), \hat{\mathbf{U}}^(t))_t\}$ with $\hat{\mathbf{X}}(t) = \mathbf{P}^\top \mathbf{X}(t)$ and $\hat{\mathbf{U}}^*(t) = \mathbf{P}^\top \mathbf{U}^*(t)$. Let $\hat{\mathcal{H}}^*$ be the optimal set of filter taps*

$$\hat{\mathcal{H}}^* = \underset{\hat{\mathcal{H}}}{\operatorname{argmin}} \sum_{(\hat{\mathbf{X}}(t), \hat{\mathbf{U}}^*(t))_t \in \hat{\mathcal{T}}} \sum_t \left\| \Phi(\hat{\mathbf{X}}(t); \hat{\mathbf{S}}, \hat{\mathcal{H}}) - \hat{\mathbf{U}}^*(t) \right\|. \quad (16)$$

Then, it holds that

$$\hat{\mathcal{H}}^* \equiv \mathcal{H}^*. \quad (17)$$

Proof. See Appendix A. \square

Thm. 1 proves that if the filter taps are optimal for a certain network, then they are optimal for all of its permutations. Note that this is the case since Thm. 1 holds for any permutation matrix \mathbf{P} , irrespective of whether we know the specific permutation, i.e. without need to compute exactly what permutation of \mathbf{S} , $\hat{\mathbf{S}}$ is. We acknowledge that it in practical instances, it may be unreasonable to expect that all the networks we observe during deployment are actually permutations of each other. However, since the filters only involve information of up to the K -hop neighborhood, transference is still successful if the graphs involved present topological symmetries within these neighborhoods. In any case, given the continuity of the problem (13) and of the chosen parametrizations Φ , we expect the transference to also be successful in instances where graphs are not exactly permutations to each other, but close. This is usually the case where graphs come from the same family (i.e. random planar graphs, Erdős-Rényi, etc.), see [25], [53].

Permutation invariance of the optimal filter taps relies on the permutation equivariance of the involved parametrizations, namely graph filters [25, Prop. 1], GCNNs [25, Prop. 2] and GRNNs [22, Prop. 1]. This property implies that the learned controllers are independent of the choice of node labeling. This an important property since, by definition, the set of nodes \mathcal{V} is unordered, and thus when we describe a graph signal in terms of a vector (a matrix) we are forcing an (arbitrary) ordering of the nodes. Stability to perturbations, on the other hand, implies that if the graph support matrix \mathbf{S} changes slightly, then the corresponding change in the output of a GCNN, operating on the same input \mathbf{X} and with the same filter taps \mathcal{H} , is bounded linearly by the size of the change in \mathbf{S} [25, Thm. 4].

In summary, the properties of permutation equivariance and stability to perturbations play a crucial role in explaining their observed scalability and transferability [53]. Permutation equivariance makes the controllers exploit the internal symmetries of the underlying graph support allowing them to speed up training and learn from fewer samples. That is, observing a specific sample from the training set and learning how to process the signal from it, immediately means that the architecture also learned how to process the signal when located at any other topologically equivalent subgraph. Stability to perturbations means that the learned architectures transfer between different physical networks as long as they are similar. This is particularly important when we expect to use the learned controller in physical network configurations unseen at training time [1], [2].

Table I: Average (std. deviation) normalized cost for different hyperparameters in the flocking problem. Optimal cost: $52(\pm 1)$.

$G \setminus K$	2	3	4	2	3	4	2	3	4
16	10(± 2)	8(± 2)	8(± 1)	3.4(± 0.3)	3.2(± 0.2)	3.1(± 0.3)	2.7(± 0.2)	2.6(± 0.1)	2.6(± 0.1)
32	11(± 3)	8(± 1)	7(± 1)	1.88(± 0.07)	1.8(± 0.1)	1.81(± 0.07)	1.60(± 0.07)	1.58(± 0.07)	1.58(± 0.07)
64	10(± 2)	8(± 1)	8(± 1)	1.6(± 0.2)	1.60(± 0.08)	1.63(± 0.08)	1.48(± 0.05)	1.48(± 0.05)	1.48(± 0.06)
(a) GF				(b) GCNN			(c) GRNN		

V. TIME-VARYING GRAPHS

The parametrizations discussed in Sec. III, while suitable to learn decentralized controllers, assume that the trajectory $\{\mathbf{X}(t)\}$ is defined always on the same graph described by \mathbf{S} . However, in many practical instances, the control actions cause a movement of the agents. Such a movement alters the relative location of the agents, and thus, alters the communication network that the agents establish. Changing the communication network means that the graph support changes and thus the graph filter (7) may no longer accurately model the communication dynamics. While there are several different graph-time filter alternatives [30], [54]–[56], in what follows we focus on *unit-delay* graph filters, and we build the corresponding *unit-delay* GCNNs and GRNNs from them.

Let $\{(\mathbf{X}(t), \mathbf{S}(t))\}$ be a *trajectory* where now each point in the sequence is comprised of a graph signal $\mathbf{X}(t)$ and its corresponding support $\mathbf{S}(t)$. Consider that each time instant t represents the *exchange clock*. This means that every time a node exchanges information with its neighbors, one time instant passes, creating a *delayed information structure* [1]

$$\mathcal{X}_i(t) = \bigcup_{k=0}^{\infty} \left\{ \mathbf{X}_j(t-k), j : v_j \in \mathcal{N}_i^k(t) \right\} \quad (18)$$

where $\mathcal{N}_i^k(t)$ is the set of nodes k hops away from node i , delayed k time instants, and defined recursively as $\mathcal{N}_i^k(t) = \{v_{j'} \in \mathcal{N}_j^{k-1}(t-1), j : v_j \in \mathcal{N}_i(t)\}$ with $\mathcal{N}_i^1(t) = \mathcal{N}_i(t)$ and $\mathcal{N}_i^0 = \{v_i\}$. The collection $\mathcal{X}(t) = \{\mathcal{X}_i(t)\}_{i=1,\dots,N}$ of the delayed information structure at all nodes is the *delayed information history*. The delayed information structure (18) means that each node only has access to past information from its neighbors, and this information gets delayed by the number of hops that had to be traversed to reach such information.

The FIR graph filter can be adapted to respect the delayed information history as follows [cf. (7)]

$$\mathbf{H}(\mathcal{X}(t)) = \sum_{k=0}^K \mathbf{S}(t) \cdots \mathbf{S}(t-(k-1)) \mathbf{X}(t-k) \mathbf{H}_k \quad (19)$$

where the set of filter taps $\mathcal{H} = \{\mathbf{H}_k, k = 0, \dots, K\}$ characterizes the operation. Note that the output of (19) is also a graph process defined over the same support sequence $\{\mathbf{S}(t)\}$ as the input graph process $\{\mathbf{X}(t)\}$. The filter in (19) is usually called a *unit-delay graph filter*.

These delayed graph filters can be used to build a *unit-delay GCNN* as follows [cf. (9)]

$$\Phi(\mathcal{X}(t)) = \sigma(\mathbf{H}(\mathcal{X}(t))) \quad (20)$$

with σ a pointwise nonlinearity. The delayed GCNN is characterized by the same set of filter taps \mathcal{H} and its output is also a graph process, but it is a nonlinear map from the input.

Likewise, we can adapt the GRNN (11)-(12) to satisfy the delayed information history. The hidden state becomes

$$\mathbf{Z}(t) = \sigma(\mathbf{A}(\mathcal{X}(t)) + \mathbf{B}(\mathbf{Z}(t-1))) \quad (21)$$

where both \mathbf{A} and \mathbf{B} are unit-delay graph filters [cf. (19)], but the second one acting on the delayed information history created by the hidden state sequence $\mathbf{Z}(t) = \{\mathbf{Z}_i(t)\}_{i=1,\dots,N}$ with $\mathbf{Z}_i(t) = \bigcup_{k=0}^{\infty} \{\mathbf{Z}_j(t-k), j : v_j \in \mathcal{N}_i^k(t)\}$ [cf. (18)]. The output is now

$$\mathbf{U}(t) = \rho(\mathbf{C}(\mathbf{Z}(t))) \quad (22)$$

with \mathbf{C} a delayed graph convolution [cf. (19)] as well. Note that since $\mathbf{U}(t)$ depends on $\mathbf{Z}(t)$ which, in turn, depends on $\mathcal{X}(t)$, then this means that the clock of the output is one time unit delayed with respect to the clock of the input.

VI. FLOCKING

In the problem of *flocking*, the objective is to coordinate a team of agents, initially flying at random velocities, to fly at the same velocity while avoiding collisions [1], [29], [57]. We use this example to illustrate the power of GCNNs [cf. (20)] and GRNNs [cf. (21)-(22)] in learning decentralized and scalable controllers.

Dynamics. We consider N agents, with $v_i \in \mathcal{V}$ described by its position $\mathbf{r}_i(t) \in \mathbb{R}^2$, its velocity $\mathbf{v}_i(t) \in \mathbb{R}^2$ and its acceleration $\mathbf{u}_i(t) \in \mathbb{R}^2$. The evolution of the system is

$$\begin{aligned} \mathbf{r}_i(t+1) &= \mathbf{u}_i(t)T_s^2/2 + \mathbf{v}_i(t)T_s + \mathbf{r}_i(t) \\ \mathbf{v}_i(t+1) &= \mathbf{u}_i(t)T_s + \mathbf{v}_i(t) \end{aligned} \quad (23)$$

for $i = 1, \dots, N$. These dynamics imply that the acceleration $\mathbf{u}_i(t)$ is held constant for the duration of the sampling interval $[tT_s, (t+1)T_s)$ and that the agents can adjust it instantaneously between sampling intervals. This is a simple model that serves as a proof-of-concept experiment of the use of GNNs to learn decentralized controllers. More involved examples can be found in [1], [58]. We set $T_s = 0.01$ s and $N = 50$ agents.

Evaluation. Formally, the objective of flocking is to determine the accelerations $\{\mathbf{U}(t)\}_t$ that make the velocities of all agents in the team be the same. We thus evaluate the performance of a given controller in terms of the velocity variation of the team

$$J(\mathbf{V}(t)) = \frac{1}{N} \sum_{i=1}^N \left\| \mathbf{v}_i(t) - \frac{1}{N} \sum_{j=1}^N \mathbf{v}_j(t) \right\|^2 \quad (24)$$

Essentially, the cost (24) is measuring how different the velocity of each individual agent $\mathbf{v}_i(t)$ is from the average velocity of the team $N^{-1} \sum_{j=1}^N \mathbf{v}_j(t)$. We note that $\sum_t J(\mathbf{V}(t))$ also measures how long it takes for the system to get controlled, while $J(\mathbf{V}(T))$ for some time horizon T gives us an idea of how good the objective was achieved in the end.

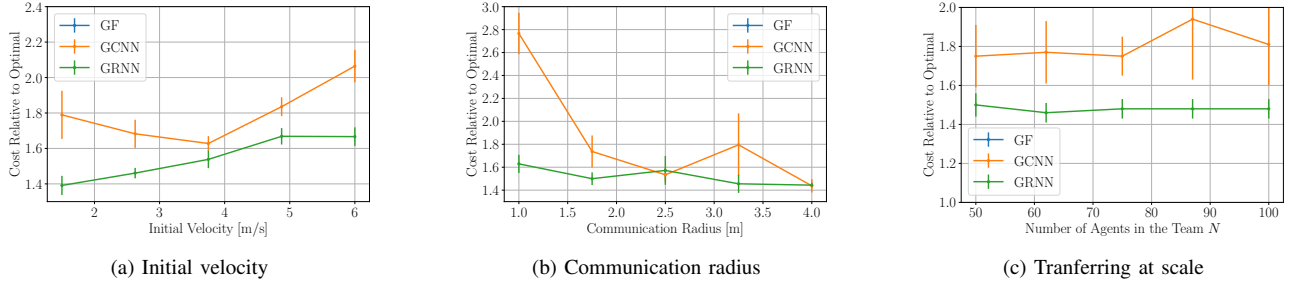


Figure 1. Change in the cost, relative to the optimal cost, for different values of (a) initial velocity, (b) communication radius, and (c) size of the team at test time (always trained on teams of size $N = 50$). The relative values of the linear graph filter controller exceed $7(\pm 1)$, $8(\pm 1)$, and $8(\pm 2)$, respectively, and thus are not shown.

Centralized controller. A *centralized* controller that avoids collisions is given by [57]

$$\mathbf{u}_i^*(t) = -\sum_{j=1}^N (\mathbf{v}_i(t) - \mathbf{v}_j(t)) - \sum_{j=1}^N \nabla_{\mathbf{r}_i} \text{CA}(\mathbf{r}_i(t), \mathbf{r}_j(t))$$

where $\nabla_{\mathbf{r}_i} \text{CA}(\mathbf{r}_i(t), \mathbf{r}_j(t))$ is the gradient of the collision avoidance potential $\text{CA} : \mathbb{R}^2 \times \mathbb{R}^2 \rightarrow \mathbb{R}$ with respect to the position of the agent v_i and evaluated at its position $\mathbf{r}_i(t)$ and the position of every other agent $\mathbf{r}_j(t)$ at time t . The specific form of the collision avoidance potential CA is given by

$$\text{CA}(\mathbf{r}_i, \mathbf{r}_j) = \begin{cases} 1/\|\mathbf{r}_{ij}\|^2 - \log(\|\mathbf{r}_{ij}\|^2) & \text{if } \|\mathbf{r}_{ij}\| \leq R_{CA} \\ 1/R_{CA}^2 - \log(R_{CA}^2) & \text{otherwise} \end{cases}$$

with $\mathbf{r}_{ij} = \mathbf{r}_i - \mathbf{r}_j$ and $R_{CA} > 0$ indicating the minimum acceptable distance between agents. Certainly, $\mathbf{u}_i^*(t)$ is a centralized controller since computing it requires agent v_i to have instantaneous knowledge of $\mathbf{v}_j(t)$ and $\mathbf{r}_j(t)$ of every other agent v_j in the team. We set $R_{CA} = 1\text{m}$.

Communication network. The communication network between agents is determined by their proximity. If agents v_i and v_j are within a communication radius R of each other then they are able to establish a link. This builds a communication graph with edge set $\mathcal{E}(t)$ such that $(v_i, v_j) \in \mathcal{E}(t)$ if and only if $\|\mathbf{r}_i(t) - \mathbf{r}_j(t)\| \leq R$. We adopt the corresponding binary adjacency matrix as the support $\mathbf{S}(t)$. We assume that communication exchanges occur within the interval determined by the sampling time T_s , so that the action clock and the communication clock coincide. We note that this is a simplified communication model, but that more involved models accounting for channel losses are possible by simply adjusting the communication graph $\mathcal{G}(t)$ and the corresponding support matrix $\mathbf{S}(t)$. We set $R = 2\text{m}$.

The state of the system $\mathbf{x}_i(t) \in \mathbb{R}^6$, which are the messages transmitted among agents, is given by [1]

$$\mathbf{x}_i(t) = \left[\begin{array}{c} \sum_{j:v_j \in \mathcal{N}_i(t)} (\mathbf{v}_i(t) - \mathbf{v}_j(t)), \\ \sum_{j:v_j \in \mathcal{N}_i(t)} \frac{\mathbf{r}_{ij}(t)}{\|\mathbf{r}_{ij}(t)\|^4}, \sum_{j:v_j \in \mathcal{N}_i(t)} \frac{\mathbf{r}_{ij}(t)}{\|\mathbf{r}_{ij}(t)\|^2} \end{array} \right]. \quad (25)$$

Note that the value of the state (25) for each agent can be computed locally, depending on the relative distance and

velocity between each agent and its immediate neighbors. Thus, the observation model (25) satisfies Assumption 1.

Decentralized learning architectures. The communication network imposes a delayed information structure $\mathcal{X}(t)$ [cf. (18)], and thus we adopt models based on unit-delay filters [cf. Sec. V]. First, we consider linear graph filters $H(\mathcal{X}(t))$ given by (19). More specifically, we consider a cascade of two filters, the first one producing $F_1 = G$ features after $K_1 = K$ communications, and the second one combining those G features into the $F_2 = 2$ output features (with $K_2 = 0$), corresponding to the control action $\mathbf{u}_i(t)$ taken by each agent. Second, a two-layer GCNN $\Phi_{\text{GCNN}}(\mathcal{X}(t))$ given by (20), with $F_1 = G$, $K_1 = K$, $F_2 = 2$, $K_2 = 0$ and a hyperbolic tangent nonlinearity $\sigma(x) = \tanh(x)$. Third, GRNNs $\Phi_{\text{GRNN}}(\mathcal{X}(t), \mathcal{Z}(t))$, with $H = G$ and K for the hidden state (21), and 2 output features and $K_o = 0$ for (22). The values of G and K are set separately for each controller as discussed in Experiment 1.

Training. The dataset is comprised of 400 trajectories for training, 20 for validation and 20 for testing. Each trajectory is generated by positioning the agents at random in a circle such that their minimum initial distance is 0.1m and their initial velocities are picked also at random from the interval $[-3, 3]\text{m/s}$ in each direction. We note that a bias velocity, also picked at random from $[-3, 3]\text{m/s}$ is included so as to avoid the flocking velocity to be zero. The trajectories are of duration 2s and the maximum acceleration is 10m/s^2 . The models are trained for 30 epochs with a batch size of at most 20 trajectories, totaling 600 training steps. Every 5 training steps, the cost (24) is evaluated on the validation set. After training has finished, we retain the model characterized by the set of parameters that has achieved the lowest cost (24) on the validation set to avoid overfitting [50, Ch. 28]. We solve the imitation learning problem (13) using the ADAM algorithm [59] with learning rate $5 \cdot 10^{-4}$ and forgetting factors 0.9 and 0.999. The loss function used for the imitation learning is the mean squared error between the output of the model and the optimal control action. The evaluation measure is the cost (24). We repeat the simulations for 10 realizations of the dataset and report the average cost as well as the standard deviation.

Experiment 1: Hyperparameter Choice. First, we test different values of features $G \in \{16, 32, 64\}$ and filter taps $K \in \{2, 3, 4\}$. Results are shown in Table I. We see that the

Table II: Average (std. deviation) evaluation measures for different hyperparameters of the learned architectures. The first column of tables shows success rate, while the second column shows the increase in flowtime.

$G \setminus K$	2	3	4
16	0.85(± 0.09)	0.85(± 0.09)	0.85(± 0.09)
32	0.84(± 0.08)	0.84(± 0.08)	0.84(± 0.08)
64	0.86(± 0.09)	0.84(± 0.08)	0.87(± 0.09)

(a) GF – Success rate

$G \setminus K$	2	3	4
16	0.87(± 0.09)	0.87(± 0.09)	0.86(± 0.09)
32	0.91(± 0.09)	0.89(± 0.09)	0.90(± 0.09)
64	0.90(± 0.09)	0.91(± 0.09)	0.89(± 0.09)

(c) GCNN – Success rate

$G \setminus K$	2	3	4
16	0.66(± 0.07)	0.74(± 0.07)	0.78(± 0.09)
32	0.83(± 0.08)	0.81(± 0.09)	0.79(± 0.08)
64	0.90(± 0.09)	0.87(± 0.09)	0.89(± 0.09)

(e) GRNN – Success rate

$G \setminus K$	2	3	4
16	0.093(± 0.009)	0.092(± 0.009)	0.090(± 0.009)
32	0.091(± 0.009)	0.093(± 0.009)	0.091(± 0.009)
64	0.092(± 0.009)	0.091(± 0.009)	0.090(± 0.009)

(b) GF – Flowtime increase

$G \setminus K$	2	3	4
16	0.087(± 0.009)	0.085(± 0.009)	0.081(± 0.008)
32	0.078(± 0.008)	0.073(± 0.007)	0.075(± 0.008)
64	0.073(± 0.009)	0.071(± 0.007)	0.071(± 0.008)

(d) GCNN – Flowtime increase

$G \setminus K$	2	3	4
16	0.10(± 0.01)	0.09(± 0.01)	0.09(± 0.01)
32	0.085(± 0.009)	0.082(± 0.008)	0.088(± 0.009)
64	0.078(± 0.008)	0.084(± 0.008)	0.088(± 0.009)

(f) GRNN – Flowtime increase

linear graph filter has a performance that is five times worse than the nonlinear architectures. This is because we know that even for simple linear problems, the optimal decentralized solution is nonlinear [15], and thus cannot be captured by a linear model. Then we see that the GRNN exhibits the best performance, and that the GCNN comes in second with reasonably good performance as well. We also observe that more features G improves performance in this range, but not necessarily larger K . From this simulation we select the best pair (G, K) for each of the three architectures and keep them for the following experiments. For these selected values, we note that, at the end time T , the velocity variation of the team [cf. (24)] is $0.0132(\pm 0.043)$ for the GCNN and $0.0116(\pm 0.0029)$ for the GRNN, showing that the team is successfully flocking together. More specifically, this is evidenced by the fact that the velocity is 0.11m/s within the average velocity of the team, which is in the order of 3m/s , thus showing less than 4% flocking error in the end.

Experiment 2: Initial conditions. Second, we run tests for different initial conditions, namely different initial velocities (Fig. 1a) and different communication radius (Fig. 1b). These experiments test the robustness of the architectures to different initial conditions. We observe in Fig. 1a that larger initial velocities implies harder to control flocks, and thus the performance decreases as the initial velocities grow. Nevertheless, the GRNN seems to be more robust than the GCNN. With respect to the communication radius, we observe in Fig. 1b that the larger the communication radius, the easier the flock is to control. This is expected since more agents can be reached and thus information travels faster with less delay. Again, the more robust architecture is the GRNN.

Experiment 3: Transfer at scale. As a third and final experiment, we run a test on transferring at scale. We train the architectures for 50 agents, but then we test them on $N \in \{50, 62, 75, 87, 100\}$ agents. Results are shown in Fig. 1c. We observe that both nonlinear architectures (GCNN and GRNN) have good scalability, with the GRNN being virtually perfect, i.e. keeping the same performance as the number of agents increases. This is due to their equivariance and stability properties [cf. Sec. IV]. In essence, this last experiment shows

that it is possible to learn a decentralized controller in a small network setting and then, once trained, transfer this solution to larger networks, without any re-training, successfully scaling.

VII. PATH PLANNING

Efficient and collision-free path planning in multi-agent systems is fundamental to advancing mobility. The overarching aim is to generate jointly collision-free paths leading agents from their start positions to designated goal positions. In the discrete domain, this problem is generally referred to as Multi-Agent Path Finding (MAPF). Coupled centralized approaches, which consider the joint configuration space of all involved agents, have the advantage of producing optimal and complete plans, yet tend to be computationally expensive. Indeed, solving for optimality is NP-hard [60], and although significant progress has been made towards alleviating the computational load [52], [61], it still scales poorly in environments with a high number of potential path conflicts.

Dynamics. Consider a $2D$ finite grid, where agents can move to adjacent positions in the grid at every time instant, as given by a *decision clock* $t = 0, 1, \dots$. This $2D$ grid contains some positions that are blocked and to which the agents cannot access. These positions are called *obstacles* and an agent attempting to move into such a position would incur in a *collision*. Each agent can only partially observe the immediate grid, as given by a rectangle of size $W_{\text{FOV}} \times H_{\text{FOV}}$, centered at the agent. They further know the relative direction of the target. What is important to realize here, is that the perception of each agent, that is, the local state, does not involve any global information, and thus satisfies Asn. 1. At every instant of the decision clock, the agents take an action $\mathbf{u}_i(t)$, moving into one of the four adjacent positions in the grid (or deciding to stay put), with the objective of moving towards its goal on a collision-free path. Note that there are only 5 possible actions (a discrete action space). We thus formulate the multi-agent path planning problem as a sequential decision-making problem [2], [62]. We consider $N = 10$ agents, navigating a 20×20 grid with a 15% obstacle density.

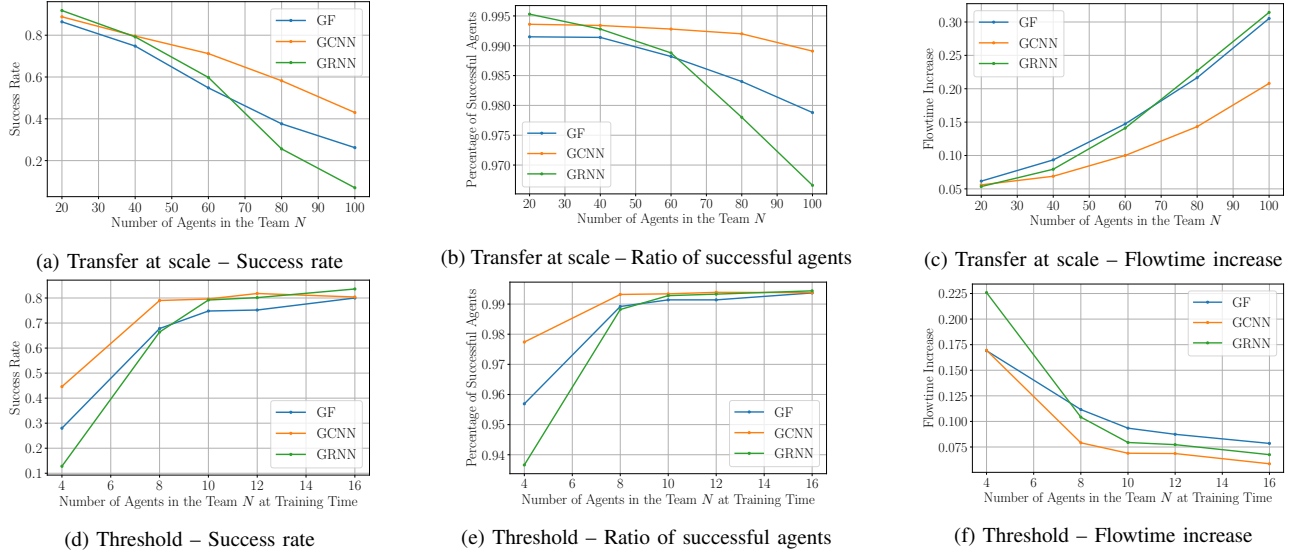


Figure 2. Experiments about transferring at scale. The learning architectures are trained on a 20×20 map with 10 agents and tested on a 50×50 map with the number of agents indicated. (a) Success rate: number of cases in the test set where *all* agents arrive at their goal. (b) Ratio of successful agents (ratio of agents that arrive at their goal). (c) Increase in flowtime.

Evaluation. We measure the performance following two metrics. First, the *success rate* α given by the ratio of successful cases over the total number of tested cases. We consider a case to be successful if *all* of its agents have arrived at their destinations before the set timeout. Second, we use the flowtime increase δ_{FT} , which measures the excess time that takes to complete the objective FT , relative to the time taken by the centralized controller FT^* , that is $\delta_{FT} = (FT - FT^*)/FT^*$.

Centralized controller. To learn the decentralized controllers by means of imitation learning [cf. (13)], we utilize a centralized controller $U^*(t)$ called Conflict-Based Search (CBS) [52]. CBS finds a solution by doing tree-based search on the space of possible paths, resulting in a computationally costly controller. It is then used only at training time to generate the optimal path for each agent.

Communication network. As is the case in Sec. VI, the communication network is given by a graph $\mathcal{G}(t) = (\mathcal{V}, \mathcal{E}(t))$, where two agents are able to communicate between themselves if they are close, i.e. $(v_i, v_j) \in \mathcal{E}(t)$ if and only if $\|\mathbf{r}_i(t) - \mathbf{r}_j(t)\| \leq R$, with $\mathbf{r}_i(t)$ the position of agent i at time t , and for some communication radius R . We adopt the binary adjacency matrix $\mathbf{S}(t)$ as the shift operator. We note that, unlike Sec. VI, for each time t that represents the decision clock, there can be arbitrarily many communications exchanges. That is, the communication clock can be arbitrarily faster than the decision clock. This makes sense in the current problem, since for each decision, the agents move one position in the grid, and can wait statically until they make the following decision.

Decentralized learning architectures. We consider a joint learning architecture whereby each agent processes the local map by means of a regular CNN, and then uses the resulting features as input to a decentralized architecture, i.e. a graph filter, a GCNN or a GRNN. In short, by jointly training both architectures, the system learns to extract the best features as

it pertains the communication network between the agents. Note that, since the decision clock t is slower than the communication clock, then the implementation of a graph filter can be done as in (7), for each time instant t . The CNN consists of five layers, all having filters with a kernel of size 3 with unit stride and zero-padding, followed by a ReLU nonlinearity $\sigma(x) = \max\{0, x\}$; a max pooling of size 2 is used in the odd-numbered layers. Then, for the decentralized controller, we consider first, a linear graph filter with two filters, one consisting of $F_1 = G$ features and $K_1 = K$ hops, and the second layer is the readout layer with $F_2 = 5$ and $K_2 = 0$. The second decentralized learning architecture is the two-layer GCNN with $F_1 = G$, $K_1 = K$, $F_2 = 5$ and $K_2 = 0$; and with $\sigma(x) = \tanh(x)$. Finally, the third model is a GRNN with $H = G$ and K for the hidden state (21), and 2 output features and $K_o = 0$ for (22). The values of G and K are set separately for each controller as discussed in Experiment 1.

Training. We instantiate 600 different maps, using 420 for training, 90 for validation, and 90 for testing. For each map, we generate 50 cases of placement of agents and targets. This generative process is done at uniformly at random. The models are trained for 150 epochs with a batch size of 64. We solve the imitation learning problem considering a cross-entropy loss function between the learned controller and the centralized one, since we have only 5 possible actions. We use the ADAM algorithm with learning rate that decays from 10^{-3} to 10^{-6} following a cosine annealing, and forgetting factors of 0.9 and 0.999, respectively. We also add a L_2 regularization to the trained parameters with a penalty of 10^{-5} . During training, we consider that the trajectories are updated following an online expert [2], whereby, on every validation step, we add 500 new trajectories to the training set – each trajectory obtained by using the controller learned up to that point, and then correcting them by means of the centralized controller.

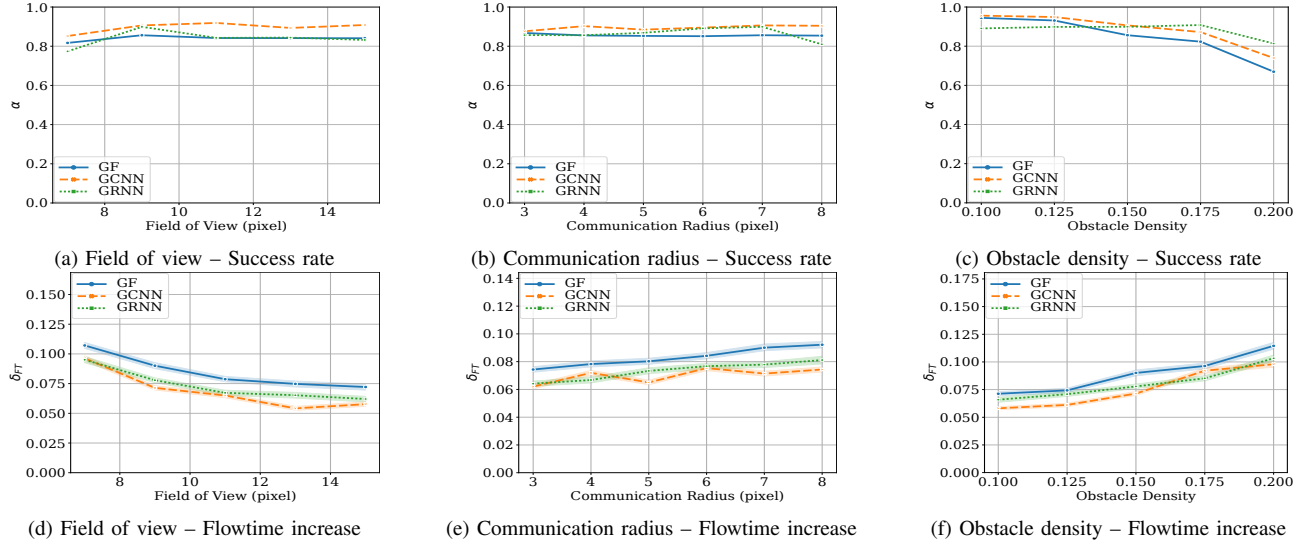


Figure 3. Top: Change in the success rate α for different values of (a) field of vision, (b) communication radius, and (c) obstacle density. Bottom: Change in flow time increase δ_{FT} , for different values of (d) field of view, (e) communication radius, and (f) obstacle density.

Experiment 1: Hyperparameter Choice. First, we test different values of features $G \in \{16, 32, 64\}$ and filter taps $K \in \{2, 3, 4\}$. Results are summarized in Table. II. Similar to flocking, we see that the performance of the linear graph filter is worse than the nonlinear architectures based on the GCNN and GRNN, both in terms of success rate and flowtime increase. Unlike flocking, however, we see that the GCNN exhibits the best performance. This could be explained due to the fact that the communication clock and the decision clock are different. That is, since the GCNN is capable of capturing several hop information before the graph changes, it does not suffer from quick topology changes. Also, the nature of path planning is likely to rely more on current and future steps rather than previous steps (historical information). We also observe that the performance of the GRNN is highly sensitive to changes in the hyperparameter choice G and K . From this simulation, we select the best pair (G, K) for each of the three architectures and keep them for the following experiments; namely, $G = 64, K = 4$ for the graph filter, $G = 64, K = 3$ for the GCNN, and $G = 64, K = 2$, for the GRNN.

Experiment 2: Initial conditions. Second, we run tests for different initial conditions, namely different field of view size, different communication radius and different obstacle density in the environment. Results are shown in Fig. 3. These experiments test the robustness of the architectures to a wider range of setups. First, we observe in Figs. 3a and 3d that a bigger field of view leads to improved performance, both in terms of the success rate and the flowtime increase. This is because each agent has immediate access to more information about the environment and can thus improve its decisions based on this. We note that the GCNN seems to be more robust than the GRNN. When changing the communication radius, we observe in Fig. 3b that an increased communication radius improves the success rate slightly (for the GCNN and the GRNN) likely because more information is used to make a decision. However, as observed in Fig. 3e, increasing

the communication radius may cause redundant information exchanges, resulting in higher increase in the flowtime. Finally, we consider different obstacles densities, with results shown in Figs. 3c and 3f. In this last case, as the obstacle density in the environment increases, the path planning becomes increasingly challenging, as evidence in the decrease on the success rate (Fig. 3c) and the increase in the flowtime (Fig. 3f). Interestingly, the GRNN becomes better, relatively speaking, as the obstacle density increases. This could be explained by the fact that more obstacles implies more landmarks that can be memorized to assist navigation.

Experiment 3: Transfer at scale. Finally, we carried out the experiment on transferring at scale. Namely, we train the architectures on a 20×20 map with 10 agents, and then we test it on a 50×50 map with an increasing number of agents $N \in \{20, 40, 60, 80, 100\}$, while maintaining the same obstacle density. We see the results in Fig. 2. The success rate (Fig. 2a) decreases considerably as the number of agents increases. Yet, it is still reasonable for 40 agents (a team four times larger than at training time). However, recall that the success rate considers the number of cases where *all* the agents reach their goal. When we, instead, look at the ratio of agents that are successful (Fig. 2b), then we see that the architectures scale well, with more than 97% of the agents reaching their goal when testing on a team with 100 agents (ten times the size of the team at training time). With respect to the increase in flowtime (Fig. 2c), we observe a similar behavior, in that up to 40 agents the learning architectures scale successfully. To complement these insights, we run a final experiment where we set the testing team size to $N = 40$ agents, and we train on teams of increasingly larger size $N \in \{4, 8, 10, 12, 16\}$. The results in Figs. 2d-2f show a thresholding effect when transferring at scale. It is evident there seems to be a minimum number of agents to scale properly, and after that number, adding more agents at training time does not necessarily improve performance.

VIII. CONCLUSIONS

The problem of controlling dynamical systems comprised of multiple autonomous agents, resides in the difficulty to find optimal controllers that respect the decentralized nature of the system. We postulate the use of graph neural networks as appropriate parametrizations for such controllers. Then, the problem reduces to finding the optimal set of parameters, finding the best possible controller within the space of graph neural networks.

Graph neural networks, in particular, graph convolutional neural networks and graph recurrent neural networks, exhibit several desirable properties in the context of decentralized control. Most importantly, they are naturally distributed and local operations, thus adapting seamlessly to the information structure imposed by the decentralized dynamical system. They are also capable of learning nonlinear behaviors which, knowing that most optimal controllers are nonlinear, becomes a relevant feat. Furthermore, both architectures are permutation equivariant and stable to changes in the graph. We then proved that, under an appropriate choice of description for the observations, this implies that the problem is permutation invariant, meaning that the same learned parameters are useful in a wide range of similar problems. Together, these properties warrant the scalability and transferability of the learned controllers.

We have tested the learned controllers in two proof-of-concept problems, namely, flocking and path planning. In both cases, we observed that the graph neural network controllers exhibit better performance than linear, decentralized controllers. More importantly, we showed the capabilities of these controllers to be deployed in larger environments. In the problem of flocking, controllers trained on a small team of 50 agents work perfectly well in teams of at least 100 agents, doubling the size; while in the problem of path planning, controllers trained in as little as 10 agents are successful in teams of 40 agents, adapting to a fourfold increase.

Overall, the proposed framework has shown promising results in simple, but useful settings. Moving forward, we expect to test graph neural networks as parametrizations in more complex control problems, investigating the impact and limitations of this choice. We further expect to develop more useful properties of these architectures as they pertain to the decentralized control problem.

APPENDIX A

PERMUTATION INVARIANCE

Proof of Theorem 1. To prove (17) we need to prove that the objective functions in (15) and (16) are equivalent. Let us start with the objective function in (16)

$$\left\| \Phi(\mathbf{P}^\top \mathbf{X}(t); \mathbf{P}^\top \mathbf{S} \mathbf{P}, \mathcal{H}) - \mathbf{P}^\top \mathbf{U}^*(t) \right\| \quad (26)$$

where we have replaced $\hat{\mathbf{X}}$, $\hat{\mathbf{S}}$ and $\hat{\mathbf{U}}$ by the corresponding definitions. We know that Φ is permutation equivariant as long as it is a graph filter [25, Prop. 1], a GCNN [25, Prop. 2] or a GRNN [22, Prop. 1], which means that

$$\Phi(\mathbf{P}^\top \mathbf{X}; \mathbf{P}^\top \mathbf{S} \mathbf{P}, \mathcal{H}) = \mathbf{P}^\top \Phi(\mathbf{X}; \mathbf{S}, \mathcal{H}). \quad (27)$$

Using the permutation equivariance of the parametrization (27) in (26) we get

$$\begin{aligned} & \left\| \mathbf{P}^\top \Phi(\mathbf{X}(t); \mathbf{S}, \mathcal{H}) - \mathbf{P}^\top \mathbf{U}^*(t) \right\| \\ &= \left\| \mathbf{P}^\top \left(\Phi(\mathbf{X}(t); \mathbf{S}, \mathcal{H}) - \mathbf{U}^*(t) \right) \right\|. \end{aligned} \quad (28)$$

Recall that for a graph signal $\mathbf{X} \in \mathbb{R}^{N \times F}$ we have $\|\mathbf{X}\| = \sum_{f=1}^F \|\mathbf{x}_f\|$, so that

$$\begin{aligned} & \left\| \mathbf{P}^\top \left(\Phi(\mathbf{X}(t); \mathbf{S}, \mathcal{H}) - \mathbf{U}^*(t) \right) \right\| \\ &= \left\| \Phi(\mathbf{X}(t); \mathbf{S}, \mathcal{H}) - \mathbf{U}^*(t) \right\|. \end{aligned} \quad (29)$$

for any p -norm $\|\cdot\|$ since \mathbf{P} is a permutation matrix. Following (26), (28) and (29), we get that (16) yields the same objective function as (15), and that solving one or the other yields the same set of filter taps, hereby completing the proof. \square

REFERENCES

- [1] E. Tolstaya, F. Gama, J. Paulos, G. Pappas, V. Kumar, and A. Ribeiro, "Learning decentralized controllers for robot swarms with graph neural networks," in *Conf. Robot Learning 2019*, vol. 100. Osaka, Japan: Proc. Mach. Learning Res., 30 Oct.-1 Nov. 2019, pp. 671–682.
- [2] Q. Li, F. Gama, A. Ribeiro, and A. Prorok, "Graph neural networks for decentralized multi-robot path planning," in *2020 IEEE/RSJ Int. Conf. Intell. Robots Syst.* Las Vegas, NV: IEEE, 25-29 Oct. 2020.
- [3] K. Ogata, *Modern Control Engineering*, 4th ed. Upper Saddle River, NJ: Prentice-Hall, 2002.
- [4] D. Owerko, F. Gama, and A. Ribeiro, "Optimal power flow using graph neural networks," in *45th IEEE Int. Conf. Acoust., Speech and Signal Process.* Barcelona, Spain: IEEE, 4-8 May 2020, pp. 5930–5934.
- [5] D. Owerko, F. Gama, and A. Ribeiro, "Predicting power outages using graph neural networks," in *2018 IEEE Global Conf. Signal and Inform. Process.* Anaheim, CA: IEEE, 26-29 Nov. 2018, pp. 743–747.
- [6] Y. Li, R. Yu, C. Shahabi, and Y. Liu, "Diffusion convolutional recurrent neural network: Data-driven traffic forecasting," in *6th Int. Conf. Learning Representations*, Vancouver, BC, 30 Apr.-3 May 2018, pp. 1–16.
- [7] E. D. Sontag, *Mathematical Control Theory: Deterministic Finite Dimensional Systems*, 2nd ed., ser. Texts Appl. Math. New York, NY: Springer, 1998, vol. 6.
- [8] R. C. Dorf and R. H. Bishop, *Modern Control Systems*, 11th ed. Upper Saddle River, NJ: Pearson Prentice Hall, 2008.
- [9] D. P. Bertsekas, *Dynamic Programming and Optimal Control*, 3rd ed. Belmont, MA: Athena Scientific, 2005, vol. 1.
- [10] R. S. Sánchez-Peña and M. Szafer, *Robust Systems: Theory and Applications*, ser. Adaptive Learning Syst. Signal Process. Commun. Control. New York, NY: John Wiley & Sons, 1998.
- [11] A. Nedic, A. Ozdaglar, and P. A. Parrilo, "Constrained consensus and optimization in multi-agent networks," *IEEE Trans. Autom. Control*, vol. 55, no. 4, pp. 922–938, Apr. 2010.
- [12] A.-H. Mohsenian-Rad and A. Leon-Garcia, "Optimal residential load control with price prediction in real-time electricity pricing environments," *IEEE Trans. Smart Grids*, vol. 1, no. 2, pp. 120–133, Sep. 2010.
- [13] M. Chiang, C. W. Tan, D. P. Palomar, D. O'Neill, and D. Julian, "Power control by geometric programming," *IEEE Trans. Wireless Commun.*, vol. 6, no. 7, pp. 2640–2651, July 2007.
- [14] C. P. Bechlioulis and G. A. Rovithakis, "Robust adaptive control of feedback linearizable mimo nonlinear systems with prescribed performance," *IEEE Trans. Autom. Control*, vol. 53, no. 9, pp. 2090–2099, Oct. 2008.
- [15] H. S. Witsenhausen, "A counterexample in stochastic optimum control," *SIAM J. Control*, vol. 6, no. 1, pp. 131–147, 1968.
- [16] F. Gama, E. Isufi, G. Leus, and A. Ribeiro, "Graphs, convolutions, and neural networks: From graph filters to graph neural networks," *IEEE Signal Process. Mag.*, vol. 37, no. 6, pp. 128–138, Nov. 2020.
- [17] J. Bruna, W. Zaremba, A. Szlam, and Y. LeCun, "Spectral networks and deep locally connected networks on graphs," in *2nd Int. Conf. Learning Representations*, Banff, AB, 14-16 Apr. 2014, pp. 1–14.

- [18] M. Defferrard, X. Bresson, and P. Vandergheynst, "Convolutional neural networks on graphs with fast localized spectral filtering," in *30th Conf. Neural Inform. Process. Syst.* Barcelona, Spain: Neural Inform. Process. Syst. Foundation, 5-10 Dec. 2016, pp. 3844–3858.
- [19] T. N. Kipf and M. Welling, "Semi-supervised classification with graph convolutional networks," in *5th Int. Conf. Learning Representations*, Toulon, France, 24-26 Apr. 2017, pp. 1–14.
- [20] F. Gama, A. G. Marques, G. Leus, and A. Ribeiro, "Convolutional neural network architectures for signals supported on graphs," *IEEE Trans. Signal Process.*, vol. 67, no. 4, pp. 1034–1049, 15 Feb. 2019.
- [21] Y. Seo, M. Defferrard, P. Vandergheynst, and X. Bresson, "Structured sequence modeling with graph convolutional recurrent networks," in *32nd Conf. Neural Inform. Process. Syst.* Montreal, QC: Neural Inform. Process. Syst. Foundation, 3-8 Dec. 2018, pp. 362–373.
- [22] L. Ruiz, F. Gama, and A. Ribeiro, "Gated graph recurrent neural networks," *IEEE Trans. Signal Process.*, vol. 68, pp. 6303–6318, 26 Oct. 2020.
- [23] E. Isufi, F. Gama, and A. Ribeiro, "EdgeNets: Edge varying graph neural networks," *arXiv:2001.07620v2 [cs.LG]*, 12 March 2020. [Online]. Available: <http://arxiv.org/abs/2001.07620>
- [24] L. Ruiz, F. Gama, A. G. Marques, and A. Ribeiro, "Invariance-preserving localized activation functions for graph neural networks," *IEEE Trans. Signal Process.*, vol. 68, pp. 127–141, 25 Nov. 2019.
- [25] F. Gama, J. Bruna, and A. Ribeiro, "Stability properties of graph neural networks," *IEEE Trans. Signal Process.*, vol. 68, pp. 5680–5695, 25 Sep. 2020.
- [26] S. Pfommer, F. Gama, and A. Ribeiro, "Discriminability of single-layer graph neural networks," *arXiv:2010.08847v2 [eess.SP]*, 21 Oct. 2020. [Online]. Available: <http://arxiv.org/abs/2010.08847>
- [27] S. Ross and J. A. Bagnell, "Efficient reductions for imitation learning," in *13th Int. Conf. Artificial Intell., Statist.* Sardinia, Italy: Proc. Mach. Learning Res., 13-15 May 2010, pp. 661–668.
- [28] S. Ross, G. J. Gordon, and J. A. Bagnell, "A reduction of imitation learning and structured prediction to no-regret online learning," in *14th Int. Conf. Artificial Intell., Statist.* Fort Lauderdale, FL: Proc. Mach. Learning Res., 11-13 Apr. 2011, pp. 627–635.
- [29] H. G. Tanner, "Flocking with obstacle avoidance in switching networks of interconnected vehicles," in *IEEE Int. Conf. Robotics and Automation 2004*. New Orleans, LA: IEEE, 26 Apr.-1 May 2004, pp. 3006–3011.
- [30] F. Gama, E. Isufi, A. Ribeiro, and G. Leus, "Controllability of bandlimited graph processes over random time varying graphs," *IEEE Trans. Signal Process.*, vol. 67, no. 24, pp. 6440–6454, 15 Dec. 2019.
- [31] S. Fattahi, N. Matni, and S. Sojoudi, "Efficient learning of distributed linear-quadratic controllers," *arXiv:1909.09895v2 [math.OC]*, 11 Oct. 2019. [Online]. Available: <http://arxiv.org/abs/1909.09895>
- [32] F. Gama and S. Sojoudi, "Graph neural networks for distributed linear-quadratic control," *arXiv:2011.05360v2 [eess.SY]*, 13 Nov. 2020. [Online]. Available: <http://arxiv.org/abs/2011.05360>
- [33] L. Ruiz, F. Gama, and A. Ribeiro, "Graph neural networks: Architectures, stability and transferability," *arXiv:2008.01767v1 [cs.LG]*, 4 Aug. 2020. [Online]. Available: <http://arxiv.org/abs/2008.01767>
- [34] A. Sandryhaila and J. M. F. Moura, "Discrete signal processing on graphs," *IEEE Trans. Signal Process.*, vol. 61, no. 7, pp. 1644–1656, 1 Apr. 2013.
- [35] D. I. Shuman, S. K. Narang, P. Frossard, A. Ortega, and P. Vandergheynst, "The emerging field of signal processing on graphs: Extending high-dimensional data analysis to networks and other irregular domains," *IEEE Signal Process. Mag.*, vol. 30, no. 3, pp. 83–98, May 2013.
- [36] A. Ortega, P. Frossard, J. Kovačević, J. M. F. Moura, and P. Vandergheynst, "Graph signal processing: Overview, challenges and applications," *Proc. IEEE*, vol. 106, no. 5, pp. 808–828, May 2018.
- [37] A. Heimowitz and Y. C. Eldar, "A unified view of diffusion maps and signal processing on graphs," in *2017 Int. Conf. Sampling Theory and Appl.* Tallin, Estonia: IEEE, 3-7 July 2017, pp. 308–312.
- [38] P. P. Vaidyanathan, *Multirate Systems and Filter Banks*. Englewood Cliffs, NJ: Prentice-Hall, 1993.
- [39] G. Mateos, S. Segarra, A. G. Marques, and A. Ribeiro, "Connecting the dots: Identifying network structure via graph signal processing," *IEEE Signal Process. Mag.*, vol. 36, no. 3, pp. 16–43, May 2019.
- [40] J. Bergstra and Y. Bengio, "Random search for hyper-parameter optimization," *J. Mach. Learning Res.*, vol. 13, pp. 281–305, Feb. 2012.
- [41] K. Xu, W. Hu, J. Leskovec, and S. Jegelka, "How powerful are graph neural networks?" in *7th Int. Conf. Learning Representations*, New Orleans, LA, 6-9 May 2019, pp. 1–17.
- [42] Y. LeCun, Y. Bengio, and G. Hinton, "Deep learning," *Nature*, vol. 521, no. 7553, pp. 85–117, May 2015.
- [43] I. Goodfellow, Y. Bengio, and A. Courville, *Deep Learning*, ser. Adaptive Comput. Mach. Learning. Cambridge, MA: The MIT Press, 2016.
- [44] S. Chen, R. Varma, A. Sandryhaila, and J. Kovačević, "Discrete signal processing on graphs: Sampling theory," *IEEE Trans. Signal Process.*, vol. 63, no. 24, pp. 6510–6523, 15 Dec. 2015.
- [45] A. G. Marques, S. Segarra, G. Leus, and A. Ribeiro, "Sampling of graph signals with successive local aggregations," *IEEE Trans. Signal Process.*, vol. 64, no. 7, pp. 1832–1843, 1 Apr. 2016.
- [46] B. Girault, P. Gonçalves, and E. Fleury, "Translation and stationarity for graph signals," *École Normale Supérieure de Lyon, Inria Rhône-Alpes*, Research Report RR-8719, Apr. 2015.
- [47] N. Perraudin and P. Vandergheynst, "Stationary signal processing on graphs," *IEEE Trans. Signal Process.*, vol. 65, no. 13, pp. 3462–3477, 1 July 2017.
- [48] A. G. Marques, S. Segarra, G. Leus, and A. Ribeiro, "Stationary graph processes and spectral estimation," *IEEE Trans. Signal Process.*, vol. 65, no. 22, pp. 5911–5926, 15 Nov. 2017.
- [49] F. Gama and A. Ribeiro, "Ergodicity in stationary graph processes: A weak law of large numbers," *IEEE Trans. Signal Process.*, vol. 67, no. 10, pp. 2761–2774, 15 May 2019.
- [50] K. P. Murphy, *Machine Learning: A Probabilistic Perspective*, ser. Adaptive Comput. Mach. Learning. Cambridge, MA: The MIT Press, 2012.
- [51] R. S. Sutton and A. G. Barto, *Reinforcement Learning: An Introduction*, 2nd ed., ser. Adaptive Comput. Mach. Learning. Cambridge, MA: The MIT Press, 2018.
- [52] G. Sharon, R. Stern, A. Felner, and N. R. Sturtevant, "Conflict-based search for optimal multi-agents pathfinding," *Artificial Intell.*, vol. 219, pp. 40–66, Feb. 2015.
- [53] L. Ruiz, L. F. O. Chamon, and A. Ribeiro, "Graphon neural networks and the transferability of graph neural networks," *arXiv:2006.03548v1 [cs.LG]*, 5 June 2020. [Online]. Available: <http://arxiv.org/abs/2006.03548>
- [54] E. Isufi, A. Loukas, A. Simonetto, and G. Leus, "Filtering random graph processes over random time-varying graphs," *IEEE Trans. Signal Process.*, vol. 65, no. 16, pp. 4406–4421, 15 Aug. 2017.
- [55] F. Grassi, A. Loukas, N. Perraudin, and B. Ricaud, "A time-vertex signal processing framework: Scalable processing and meaningful representations for time-series on graphs," *IEEE Trans. Signal Process.*, vol. 66, no. 3, pp. 817–829, 1 Feb. 2018.
- [56] E. Isufi, A. Loukas, N. Perraudin, and G. Leus, "Forecasting time series with VARMA recursions on graphs," *IEEE Trans. Signal Process.*, vol. 67, no. 18, pp. 4870–4885, 15 Sep. 2019.
- [57] H. G. Tanner, A. Jadbabaie, and G. J. Pappas, "Stable flocking of mobile agents, part II: Dynamic topology," in *42nd IEEE Conf. Decision, Control*. Maui, HI: IEEE, 9-12 Dec. 2003, pp. 2016–2021.
- [58] T.-K. Hu, F. Gama, Z. Wang, A. Ribeiro, and B. M. Sadler, "VGAI: End-to-end learning of vision-based decentralized controllers for robot swarms," *arXiv:2002.02308v1 [eess.SY]*, 6 Feb. 2020. [Online]. Available: <http://arxiv.org/abs/2002.02308>
- [59] D. P. Kingma and J. L. Ba, "ADAM: A method for stochastic optimization," in *3rd Int. Conf. Learning Representations*, San Diego, CA, 7-9 May 2015, pp. 1–15.
- [60] J. Yu and S. M. LaValle, "Structure and intractability of optimal multi-robot path planning on graphs," in *27th AAAI Conf. Artificial Intell.* Bellevue, WA: Assoc. Advancement Artificial Intell., 14-18 July 2013, pp. 1443–1449.
- [61] C. Ferner, G. Wagner, and H. Choset, "ODrM* optimal multirobot path planning in low dimensional search spaces," in *2013 IEEE Int. Conf. Robotics Automat.* Karlsruhe, Germany: IEEE, 6-10 May 2013, pp. 3854–3859.
- [62] Q. Li, W. Lin, Z. Liu, and A. Prorok, "Message-aware graph attention networks for large-scale multi-robot path planning," *arXiv:2011.13219v1 [cs.RO]*, 26 Nov. 2020. [Online]. Available: <http://arxiv.org/abs/2011.13219>